Letter | Editors' Suggestion

Fluctuation-induced supersolidity at the superfluid-solid interface

Baptiste Coquinot,* Ragheed Alhyder, Alberto Cappellaro, and Mikhail Lemeshko†
Institute of Science and Technology Austria (ISTA), Am Campus 1, 3400 Klosterneuburg, Austria

(Received 9 December 2025; revised 2 September 2026; accepted 1 October 2026; published 9 November 2026)

Supersolidity, combining superfluid and crystalline orders, has been realized in dipolar Bose-Einstein condensates by tuning interatomic interactions. Here, we show that supersolidity can also emerge from mode coupling at a superfluid-solid interface, without modifying bulk interactions and for a broad class of superfluids. Using an analytical and numerical treatment of the coupled superfluid and phonon fields, we derive the criterion for a density-modulation instability driven by interfacial coupling and dependent on dimensionality. In superfluid helium, the instability first appears at the roton mode, while in a Bose-Einstein condensate with contact interactions it can occur for a large range of wave vectors. Beyond the threshold, the ground state acquires an interfacial density modulation while the bulk remains superfluid, forming a hybrid superfluid-supersolid phase. Our results identify interfacial mode coupling as a promising route to supersolidity, enabling the simultaneous exploitation of interfacial supersolid and bulk superfluid quantum properties, as well as using the interface as a seed to nucleate bulk supersolidity.

DOI: 10.1103/xfj1-gndb

Superfluidity and supersolidity are two macroscopic manifestations of quantum mechanics. Superfluidity arises when the $U(1)$ phase symmetry of the wave function is spontaneously broken, allowing the fluid to sustain frictionless flow associated with a macroscopic phase gradient. Bosonic superfluids are now well established experimentally, both in liquid helium and in Bose-Einstein condensates (BECs) [1–4]. Extending this concept, a supersolid combines superfluid and crystalline order by further breaking continuous translational symmetry of the density, thus forming a lattice [5–7]. In helium, the existence of supersolidity remains controversial [8–12]. In particular, close to solid walls, a strong and uniform absorption leads to the formation of a triangular lattice in the first layer, which is no longer superfluid, while the next layers present supersolid features [13–17]. In BECs, supersolidity has also been investigated [18–24] and was recently achieved experimentally [25–28], in particular with dipolar BECs [29–36]. In these last systems, a finite-wave-vector roton softening produces a density modulation that remains phase coherent, stabilized by quantum fluctuations. Here, guided by this mechanism, we propose that mode coupling at a superfluid-solid interface hybridizes the superfluid quasiparticles with surface phonons of the solid and induces a softening without delicate interaction tuning. For strong enough superfluid-solid coupling, we show that this softening leads to a commensurate density wave while preserving phase rigidity, thereby enabling supersolidity at the boundary.

*Contact author: Baptiste.Coquinot@ist.ac.at
†Contact author: Mikhail.Lemeshko@ista.ac.at

Published by the American Physical Society under the terms of the Creative Commons Attribution 4.0 International license. Further distribution of this work must maintain attribution to the author(s) and the published article's title, journal citation, and DOI.

The absorption and reflection of superfluid excitations at a solid boundary have long been studied in the context of superfluid helium transport [37–42]. These processes can be recast as mode couplings between the superfluid's and solid's fluctuations, as previously established for solid-solid [43–46] and solid-liquid interfaces [47–50]. High-frequency mode coupling usually dominates attractive and repulsive forces such as the van der Waals interactions. In contrast, low-frequency quasiparticles such as phonons and rotons, which are energetically more accessible, control the friction. Such coupling enables a direct exchange of excitations across the interface and gives rise to coupled transport phenomena, such as Coulomb drag effects, which appear to be particularly promising for water-solid interfaces [51–53]. In the following, we will show that these low-frequency mode couplings not only impact the transport properties but also the ground state of the system.

In this Letter, we consider interfacial mode coupling between low-frequency density modulations and show that it can drive a supersolid phase transition in both superfluid helium and Bose-Einstein condensates. The system, sketched in Fig. 1(a), consists of a (possibly confined) superfluid layer in contact with a perfectly smooth solid, modeled as a continuous elastic medium supporting phonons. At the interface, the superfluid atoms typically experience van der Waals attraction and Pauli repulsion, which define the characteristic interatomic distance σ (typically a few angstroms) and interaction energy $\mathcal{E}_0$ (typically of the order of millielectronvolts). For simplicity, we model the interfacial interaction by the contact potential

$$V_{\rm int}(\mathbf{r}) = -\alpha\delta(\mathbf{r}), \tag{1}$$

although the formalism can also accommodate finite-range or nonlocal interactions. Here, we introduced the interfacial coupling constant $\alpha \sim \mathcal{E}_0\sigma^3$, whose precise definition depends on the form of the solid-superfluid interaction potential. For

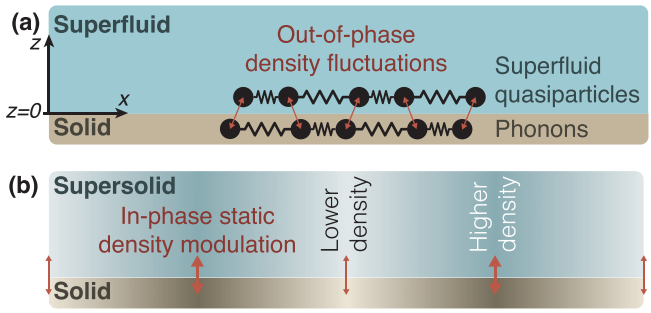


FIG. 1. Model. (a) Schematics of the system: a superfluid is deposited at a smooth solid interface. Both the superfluid and the solid have density fluctuations and they interact through an attractive coupling, but they remain uncorrelated. (b) Schematics of a supersolid phase: in order to maximize the attractive interfacial coupling, the density of both the superfluid and the solid present an in-phase density modulation in space, breaking the translation symmetry.

realistic systems, we thus expect $\alpha \sim 10^{-2} - 10^{-1}\,\mathrm{meV\,nm^3}$. Note that the coordinate origin was chosen so that the interface $z = 0$ coincides with the positions of both the first superfluid atoms and the solid surface. For uniform densities, this interaction shifts the local chemical potential at the mean-field level and may break superfluidity for strong couplings [14]. Here, we investigate whether the response of the solid may lead to density modulations with reasonable couplings. We therefore focus on density fluctuations and neglect the uniform density shift. Thus, we show that above a critical interfacial coupling strength depending on the phononic properties, the coupled densities become unstable toward an oscillatory modulation that maximizes the superfluid-solid overlap, as illustrated in Fig. 1(b).

We model the superfluid by a Gross-Pitaevskii action:

$$\mathcal{S}_{\mathrm{GP}} = \int \mathrm{d}t\,\mathrm{d}\mathbf{r}\,\psi^*(\mathbf{r},t)\left(i\hbar\partial_t + \frac{\hbar^2}{2m}\Delta + \mu\right)\psi(\mathbf{r},t) - \frac{1}{2}\int \mathrm{d}t\,\mathrm{d}\mathbf{r}\,\mathrm{d}\mathbf{r}'\,|\psi(\mathbf{r}',t)|^2 V_0(|\mathbf{r}-\mathbf{r}'|)|\psi(\mathbf{r},t)|^2, \tag{2}$$

where ψ is the superfluid order parameter, μ the chemical potential, and V_0 the interatomic interaction. The minimization of the action yields the bulk density $n_0 = \mu/\tilde{V}_0(\mathbf{q}=0)$ and we define accordingly the healing length $\xi = \hbar/\sqrt{2m\mu}$. Linearizing around the uniform solution with $\psi(\mathbf{r},t) = \sqrt{n_0 + \delta n(\mathbf{r},t)}$ yields the Bogoliubov dispersion for the low-energy density modes,

$$\mathcal{E}_{\mathrm{B}}(\mathbf{q}) = \sqrt{\mathcal{E}_{\mathrm{k}}(\mathbf{q})(\mathcal{E}_{\mathrm{k}}(\mathbf{q}) + 2\tilde{V}(\mathbf{q})n_0)}, \tag{3}$$

where $\mathcal{E}_{\mathrm{k}}(\mathbf{q}) = \hbar^2\mathbf{q}^2/2m$ is the kinetic energy. In the following, we consider either a BEC with contact interaction $V_0(\mathbf{r}) = g\delta(\mathbf{r})$ or superfluid helium where V_0 is adjusted to reproduce the experimental dispersion. On the other hand, the solid density fluctuations δn_{sol} are modeled by a Gaussian Keldysh action implementing the susceptibility $\chi^{\mathrm{R}}_{\mathrm{sol}}(\mathbf{q},\omega) = [(qc)^2/K_{\mathrm{sol}}]/[\omega^2 - 2i\gamma\omega - (qc)^2]$ corresponding to an ideal acoustic phonon with sound velocity c and damping γ. Generalization to more realistic phonon branches is straightforward. The static elastic stiffness $K_{\mathrm{sol}} = m_{\mathrm{sol}}c^2/n^0_{\mathrm{sol}}$ is obtained from the sound velocity c and the average density n^0_{sol} of atoms of mass m_{sol} on the solid surface. Details of the model and full derivations are provided in the Supplemental Material [54].

We start by considering a two-dimensional (2D) superfluid layer of thickness $\theta \ll \xi$. For small density modulations, the Gross-Pitaevskii action can be linearized into a Gaussian form around the bulk density. Including the interfacial coupling, we can compute the first-order self-energy for the superfluid density fluctuations from the product of the superfluid and solid density susceptibilities. Thus, the renormalized superfluid susceptibility reads

$$\tilde{\chi}^{\mathrm{R}}_{n^{2\mathrm{D}}}(\mathbf{q},\omega) = \frac{2\theta n_0 \mathcal{E}_{\mathrm{k}}(q)}{(\hbar\omega)^2 - \mathcal{E}_{\mathrm{B}}(q)^2 - 2\alpha^2 n_0 \mathcal{E}_{\mathrm{k}}(q)\chi^{\mathrm{R}}_{\mathrm{sol}}(\mathbf{q},\omega)/\theta}. \tag{4}$$

Then, we deduce the hybridized branches of energy for which the denominator of the renormalized susceptibility vanishes. Due to the interfacial coupling, the upper branch is energetically more costly while the lower branch is softened. When the latter becomes negative, the corresponding wave vector $\mathbf{q}$ is dynamically unstable. This happens for (see Supplemental Material [54])

$$\alpha^2 > \frac{K_{\mathrm{sol}}K_{\mathrm{GP}}(q)}{2n_0^2}, \tag{5}$$

where we introduced the stiffness of the superfluid $K_{\mathrm{GP}}(q)$, which reads for a 2D layer of thickness θ

$$K^{\mathrm{2D}}_{\mathrm{GP}}(q) = \theta n_0[\mathcal{E}_{\mathrm{k}}(q) + 2n_0\tilde{V}(q)]. \tag{6}$$

The superfluid stiffness represents the energetic cost, coming from both the kinetic energy and the interatomic interactions, of deforming the density field. We find that the instability is favored if the superfluid and the solid have a lower stiffness, corresponding to a lower energy cost for the density modulation of the supersolid phase. In particular, supersolidity is facilitated by the presence of soft solids, exhibiting slow acoustic phonons. For instance, for superfluid helium, we find reasonable values for the critical interfacial coupling constant for phonons of speed $c = 250$ m/s. Its spectral function (which highlights the branches of energy) close to the threshold is given in Fig. 2(a): the roton mode is softened and is the first mode to become unstable. Consistently, Fig. 2(b) shows for every wave vector the critical interfacial coupling required to become unstable where the minimum corresponds to the roton mode. While we may expect corrections due to the molecular structure of the solid at long wave vectors, the critical wave vector is in general incommensurate with the solid's lattice.

This mechanism is similar to the one observed in dipolar gases at the onset of supersolidity. Therefore, we can test this hypothesis by evaluating the ground-state energy using the variational ansatz $\psi(\mathbf{r},t) = \sqrt{n_0}(1 + \epsilon_0\cos(q_0 x))$ and $\delta n_{\mathrm{sol}}(\mathbf{r},t) = \epsilon_{\mathrm{sol}}\cos(q_0 x)$, where x is the in-plane direction and q_0 is a fixed wave vector. Here, we assumed a one-dimensional (1D) density modulation for simplicity, as a lattice structure would not change qualitatively our results [55]. We use the amplitude of the density modulations ϵ_0 and

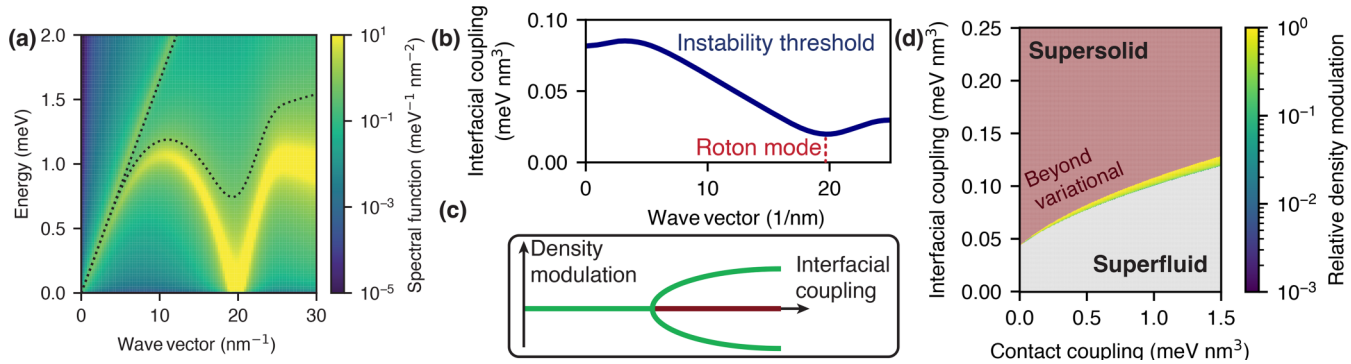


FIG. 2. Supersolid transition in two dimensions. (a) Spectral function $-\frac{1}{\pi}\mathrm{Im}[G^{\mathrm{R}}(\mathbf{q},\omega+i0^+)]$ of a 2D layer of He II renormalized by acoustic phonon of speed $c = 250$ m/s through an interfacial coupling $\alpha = 0.02$ meV nm^3. Helium has a density of $n_0 = 2.2\times10^{28}/\mathrm{m}^3$ and we use $\theta = 0.3$ nm. As an example, we use the properties of graphene in the following: an atomic density $n^0_{\mathrm{sol}} = 38/\mathrm{nm}^2$ and mass $m_{\mathrm{sol}} = 12\ m_0$ (m_0 being the atomic mass). The dashed lines correspond to the energy bands of noninteracting superfluid helium and phonons. (b) Critical interfacial coupling α to induce the supersolid instability as a function of the wave vector of the density modulation for the same system. The minimum corresponds to the roton mode. (c) Sketch of the instability bifurcation: the uniform density state becomes unstable above the interfacial coupling critical and a density modulation then becomes stable. The translation symmetry breaking results in a bifurcation. (d) Phase diagram for a 2D layer of a BEC of thickness $\theta = 1$ nm over a length $L_x = 50$ nm interacting with acoustic phonons of speed $c = 50$ m/s: relative density modulation amplitude $\epsilon_0/\sqrt{n_0}$ as a function of the contact coupling g and interfacial coupling α. The supersolid phase corresponds to a nonzero modulation. The BEC molecular mass $m = 7\ m_0$ with density $n_0 = 10^{23}/\mathrm{m}^3$.

ϵ_{sol}, which vanish in the superfluid phase and are nonzero in the supersolid phase, as variational parameters. By plugging this ansatz into the action for the whole system (superfluid and solid), we obtain the energy functional to minimize over the variational parameters. The interfacial coupling energy reads

$$\mathcal{E}_{\mathrm{el}} + \mathcal{E}_{\mathrm{int}} = \tfrac{1}{4}K_{\mathrm{sol}}\epsilon^2_{\mathrm{sol}} - \alpha n_0\epsilon_0\epsilon_{\mathrm{sol}}. \tag{7}$$

Minimizing with respect to the solid's density modulation yields $\epsilon_{\mathrm{sol}} = 2\alpha n_0 K^{-1}_{\mathrm{sol}}\epsilon_0$. Thus, the solid modulation is in phase with the superfluid's modulation. Note, however, that this modulation is independent of the solid's lattice. Plugging this into Eq. (7) and including the Gross-Pitaevskii contribution from Eq. (2) provides the effective energy cost for the superfluid which reads, up to fourth order in ϵ_0 (see Supplemental Material [54]),

$$\mathcal{E}_{\mathrm{eff}}[\epsilon_0] = \tfrac{1}{2}\big[K^{\mathrm{2D}}_{\mathrm{GP}}(q_0) - 2\alpha^2 n_0^2 K^{-1}_{\mathrm{sol}}\big]\epsilon_0^2 + \tfrac{1}{4}K^{\mathrm{2D}}_4(q_0)\epsilon_0^4, \tag{8}$$

where $K^{\mathrm{2D}}_{\mathrm{GP}}(q_0)$ is the 2D stiffness of the superfluid given in Eq. (6) and the second term describes the interfacial coupling. The quadratic coefficient becomes negative with the same threshold as in Eq. (5), signaling the transition toward a supersolid state with a density modulation. The quartic term, originating from interatomic interactions, stabilizes the density modulation and yields an analytic expression for its amplitude in the limit of small modulations. This is a standard Landau-Ginzburg functional with a pitchfork bifurcation, as sketched in Fig. 2(c), and leads to a spontaneous symmetry breaking. Above a threshold the uniform superfluid state becomes unstable while the supersolid state—with positive or negative ϵ_0 and more generally with any shift of the density modulation—becomes stable.

For a BEC with contact interactions, the stiffness $K^{\mathrm{2D}}_{\mathrm{GP}}(q_0)$ [Eq. (6)] is a growing function of the wave vector: the smallest wave vectors are therefore the easiest to destabilize. In practice in a finite size system, its length L_x selects the possible wave vectors and sets the first unstable wave vector $q_{\mathrm{min}} = 2\pi/L_x$. On the other hand, the interfacial coupling α selects the larger unstable wave vector q_{max}, which is independent from the system size L_x. Thus, all wave vectors $q_{\mathrm{min}} < q_0 < q_{\mathrm{max}}$ are linearly unstable and the resulting density profile must be determined beyond linear order. For a BEC with finite-range or nonlocal interactions, an intrinsic length scale may provide a preferred modulation wave vector, similarly to the roton softening for helium. The critical coupling [Eq. (5)] to excite a wave vector q_0 reads (see Supplemental Material [54])

$$\alpha_c = \frac{\hbar}{2}\sqrt{\frac{\theta K_{\mathrm{sol}}}{n_0 m}\big(q_0^2 + 2\xi^{-2}\big)}. \tag{9}$$

For a BEC, the density n_0 is smaller than for superfluid helium, leading to a weaker superfluid-solid interaction and therefore a higher threshold. The resulting phase diagram in Fig. 2(d), computed with a softer solid ($c = 50$ m/s), shows the boundary between superfluid and supersolid phases as a function of the interfacial coupling α, which drives the instability, and the interaction coupling g, which tends toward density uniformity. For wavelengths larger than the healing length, the critical interfacial coupling scales with $\alpha_c \propto \xi^{-1} \propto g^{1/2}$. Thus, the stronger the interatomic interaction, the harder it is to destabilize the density.

In the presence of a phase twist $\mathcal{Q}$ along the x direction, we take the order-parameter ansatz $\psi(\mathbf{r},t) = \sqrt{n_0}(1 + \epsilon_0\cos(q_0x))e^{i\mathcal{Q}x + i\phi(\mathbf{r})}$, where $\phi(\mathbf{r})$ is periodic and ensures current conservation, $\boldsymbol{\nabla}\cdot[n(\mathbf{r})(\mathcal{Q} + \boldsymbol{\nabla}\phi(\mathbf{r})] = 0$. Minimization of the energy yields the same transition as in the absence of the twist. The quadratic energy cost associated with the twist defines the superfluid phase stiffness (see Supplemental Material [54]),

$$D^{\mathrm{2D}} = \partial^2_{\mathcal{Q}}[\mathcal{E}(\mathcal{Q}) - \mathcal{E}(0)]|_{\mathcal{Q}=0} = \frac{\hbar^2 n_0}{m}\big(1-\epsilon_0^2\big)^{3/2}, \tag{10}$$

which is independent of the specific form of the interaction potential V. The corresponding superfluid fraction is

$$f_s^{2D} = \frac{mD^{2D}/\hbar^2}{\langle n(\mathbf{r})\rangle_{\mathbf{r}}} = \frac{\left(1-\epsilon_0^2\right)^{3/2}}{1+\epsilon_0^2/2}. \tag{11}$$

Thus, f_s^{2D} decreases continuously from unity as the density modulation develops but remains positive throughout the regime of validity of the variational approach.

Let us now turn to a three-dimensional (3D) system: we consider a half-space superfluid at the solid interface. We likewise expect an interfacial instability toward a density modulation which decays far from the interface. Therefore, we evaluate the ground-state energy using the same variational ansatz where the superfluid density modulation amplitude $\epsilon(z)$ is now a function of the distance to the interface z. Fixing $\epsilon(z=0)=\epsilon_0$, we expect the density modulation amplitude to decay over a skin length $\ell(q_0)$, which replaces the physical thickness θ of the 2D system. Its precise form is obtained by minimizing the Gross-Pitaevskii energy cost, which then reduces to

$$\mathcal{E}_{\mathrm{GP}}[\epsilon] = \tfrac{1}{2}K_{\mathrm{GP}}^{3D}(q_0)\,\epsilon_0^2 + \tfrac{1}{4}K_4^{3D}(q_0)\,\epsilon_0^4, \tag{12}$$

where K_{GP}^{3D} is now the 3D stiffness of the superfluid and the stabilizing quartic terms arises from interatomic interactions (see Supplemental Material [54]).

For a BEC with contact interaction, we find that the density modulation amplitude decays exponentially as $\epsilon(z)=\epsilon_0\exp(-z/\ell(q_0))$, where the skin length is $\ell(q_0)=1/\sqrt{q_0^2+2\xi^{-2}}$. For short wavelengths, the gradients of density are large and therefore the kinetic term dominates the energy cost, which is minimized by a short thickness $\ell(q_0)\approx 1/q_0$. For long wavelengths, however, the interatomic interactions are dominant and the slowly varying density modulation decays over the usual healing length $\ell(q_0)\approx\xi/\sqrt{2}$. Finally, we obtain the associated 3D stiffness $K_{\mathrm{GP}}^{3D}(q_0)=\hbar^2 n_0/2m\ell(q_0)$, which corresponds to the 2D stiffness of a layer of thickness $\ell(q_0)$. Since the effective thickness depends on the parameters of the supersolid, the scalings are different. In particular, for long wavelengths the stiffness is less sensitive to the interatomic interaction, $K_{\mathrm{GP}}^{3D}\propto g^{1/2}$, because the thickness of the modulations then shrinks.

For a generic potential V_0 (e.g., our model of superfluid helium), we similarly assume an exponential decay $\epsilon(z)=\epsilon_0\exp(-z/\ell)$ and determine $\ell(q_0)$ by minimizing the stiffness $K_{\mathrm{GP}}^{3D}(q_0,\ell)$ numerically. Including the interfacial contributions, the effective energy cost is again a Landau-Ginzburg functional and the instability threshold is still given by Eq. (5), in which the superfluid stiffness is now 3D. Figure 3(a) shows the critical interfacial coupling as a function of the wave vector for superfluid helium. We again find an instability for reasonable interfacial couplings and first for the roton mode.

For a BEC, the resulting phase diagram in Fig. 3(b) shows the boundary between superfluid and supersolid phases, with critical coupling

$$\alpha_c = \frac{\hbar}{2}\sqrt{\frac{K_{\mathrm{sol}}}{n_0 m}}\left(q_0^2+2\xi^{-2}\right)^{1/4}. \tag{13}$$

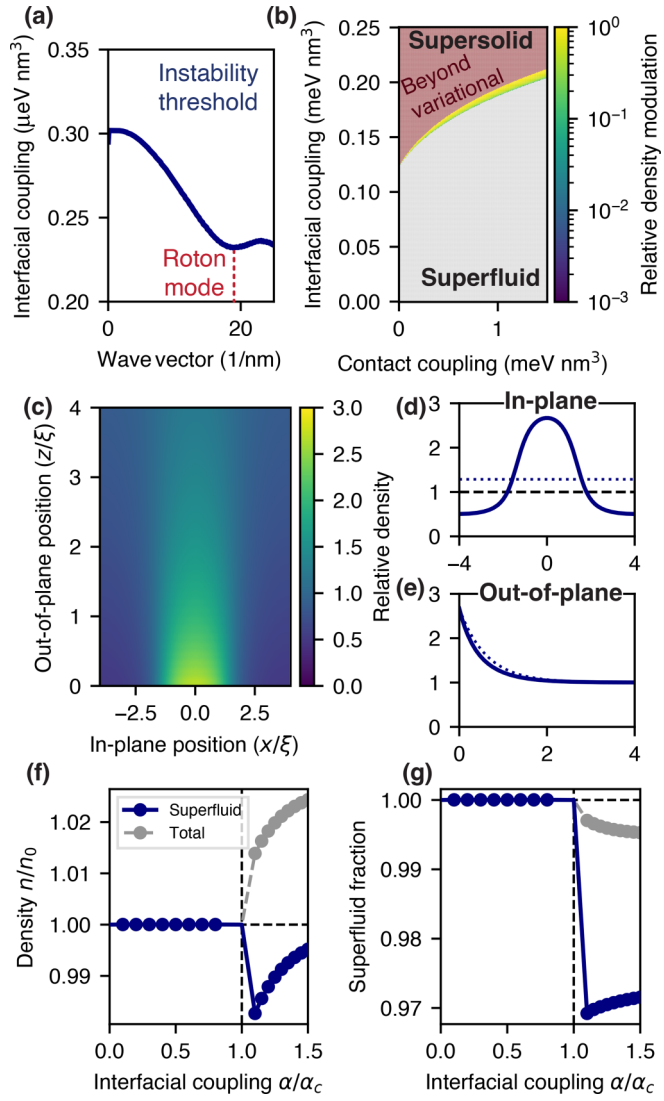


FIG. 3. Supersolid transition in three dimensions. (a) Critical interfacial coupling α for the supersolid instability vs modulation wave vector for He II coupled to acoustic phonons with $c=250$ m/s. The minimum occurs at the roton mode. (b) Phase diagram of a BEC of length $L_x=50$ nm coupled to acoustic phonons with $c=50$ m/s: relative modulation amplitude $\epsilon_0/\sqrt{n_0}$ vs contact coupling g and interfacial coupling α. The supersolid phase corresponds to a nonzero modulation. (c) Ground-state density n/n_0 of a BEC for $\alpha=1.1,\alpha_c$, obtained from numerical imaginary-time evolution of the Hamiltonian, with $g=0.75$ meV nm^3, $\alpha_c\approx 0.16$ meV nm^3, $\xi\approx 6.3$ nm, and $L_x=8\xi=50$ nm. (d) Interfacial density profile vs in-plane distance x/ξ. Blue and black dashed lines indicate the mean interfacial and bulk densities, respectively. (e) Density profile normal to the interface at $x=0$ vs z/ξ. The dashed line shows the exponential decay predicted in the small-modulation regime. (f) Total and superfluid density, extracted from the phase stiffness, vs interfacial coupling. (g) Corresponding superfluid fraction. The dashed line corresponds to the upper bound $1/\langle n(\mathbf{r})\rangle_{\mathbf{r}}\langle\langle n(\mathbf{r})\rangle_{yz}^{-1}\rangle_x$ [6].

For wavelengths larger than the healing length, the critical interfacial coupling scales with $\alpha_c\propto g^{1/4}$, a weaker scaling than in two dimensions. Nevertheless, the condition $\theta\ll\xi$ ensures that the supersolid instability in three dimensions is

less favorable than in two dimensions, due to the out-of-plane gradient cost.

In the presence of a phase twist, the same variational treatment yields the superfluid phase stiffness and the corresponding superfluid fraction. Unlike in two dimensions, the latter depends on the system size L_z normal to the interface but remains positive in all cases.

To prove that the ground state of the system is indeed a supersolid phase beyond the small modulation regime, we compute numerically the ground state of a BEC coupled to the interface by minimizing the total energy (see Supplemental Material [54]). Integrating out the solid density modulation ϕ, the interfacial coupling appears as a Robin boundary condition for the bulk Gross-Pitaevskii functional,

$$\frac{\hbar^2}{2m}\partial_z\psi|_{z=0} = -\frac{\alpha^2}{K_{\rm sol}}\,\delta|\psi|^2\,\psi|_{z=0}, \tag{14}$$

where $\delta|\psi|^2$ is the deviation of the interfacial superfluid density from its average, removing the uniform attraction that is not relevant here. For strong interfacial couplings, we find a collapse of the superfluid order parameter that focuses at the boundary. Because this is an interfacial effect, the Lee-Huang-Yang corrections [56,57] are not enough to stabilize the superfluid, thus we do not include these higher-order terms. However, in practice, the solid cannot accommodate unlimited density accumulation, therefore the right-hand-side term saturates for large superfluid densities. We thus implement a smooth saturation of the boundary condition in order to avoid any collapse. At a distance far from the interface $z = z_{\rm max}$, that is, far from the interface, the superfluid is homogeneous and thus we impose its density as $\psi(z_{\rm max}) = \sqrt{n_0}$. We choose the system size L_x in order to investigate the wave vector $q_0 = 2\pi/L_x$ and set the range of the interfacial couplings in order to excite only q_0.

Starting from an initial state that breaks translation symmetry, we then perform an imaginary-time evolution of the Gross-Pitaevskii equation in order to determine the ground state. As expected, for interfacial couplings below the threshold, the initial density modulation disappears and we find the ground state to be uniform. However, above the threshold the density modulation stabilizes with a cosinusoid-like shape, as shown in Fig. 3(c). Figure 3(d) shows the in-plane interfacial density modulation, which corresponds to the first harmonics of the system, while Fig. 3(e) displays its out-of-plane decay, which is similar to the exponential decay derived for small modulations. In the absence of a phase twist, the order parameter remains globally phase coherent. Upon imposing a small phase twist $\mathcal{Q}$, the phase acquires an additional periodic component that ensures current conservation while preserving global coherence. Numerically, the corresponding increase in the ground-state energy scales quadratically with $\mathcal{Q}$, allowing us to extract the superfluid phase stiffness and the associated superfluid density and fraction [see Figs. 3(f)–3(g)]. These quantities remain constant below the critical interfacial coupling and decrease once the density-modulated phase emerges, while remaining positive throughout the parameter range considered. As anticipated, the ground state of the system therefore corresponds to a superfluid phase below the threshold and a supersolid phase above it.

In conclusion, we have shown within a mean-field framework that the elastic response of a smooth interface can promote the transition from a superfluid to a supersolid state. While this coarse-grained description calls for future validation through more advanced numerical approaches such as quantum Monte Carlo (QMC), it isolates a feedback mechanism of the solid that has not been explored in this context [8,14,58–61]. Our results therefore suggest an alternative route to realizing supersolids experimentally, based on engineering internal wall properties rather than relying on surface roughness or strong interfacial attraction. Realizing this scenario experimentally requires a soft solid, supporting slow phonons, and a reasonable interfacial coupling between the solid and the superfluid. Both conditions might be attainable, for instance, by engineering metamaterials [62,63] and controlling the solid-superfluid attraction [64,65]. While we have assumed $T = 0$ throughout this paper, incorporating finite-temperature phonon effects would offer a natural and experimentally relevant extension of this mechanism. Moreover, our model predicts supersolidity as an interfacial phenomenon while the bulk remains superfluid. For helium films, this mechanism may contribute to the phase of the first layers [13–17]. This mixed state could combine the advantages of both phases and their mutual coupling, reminiscent of the cross-term effects between interfacial and bulk transport observed, for example, in classical nanofluidics [66]. It could also serve as a seed for bulk supersolid formation by lowering the barrier of the phase transition thanks to an interfacial nucleation.

B.C. acknowledges support from the NOMIS Foundation. R.A. acknowledges funding from the Austrian Academy of Science ÖAW Grant No. PR1029OEAW03.

Data availability. There are no publicly available research data or software supporting this manuscript. Requests for further information or data should be sent to the authors.

[1] A. Griffin, D. W. Snoke, and S. Stringari, *Bose-Einstein Condensation* (Cambridge University, Cambridge, 1996).

[2] F. Dalfovo, S. Giorgini, L. P. Pitaevskii, and S. Stringari, Theory of Bose-Einstein condensation in trapped gases, Rev. Mod. Phys. **71**, 463 (1999).

[3] H. R. Glyde, Excitations in the quantum liquid ^{4}He: A review, Rep. Prog. Phys. **81**, 014501 (2018).

[4] W. P. Halperin, Eighty years of superfluidity, Nature (London) **553**, 413 (2018).

[5] D. J. Thouless, The flow of a dense superfluid, Ann. Phys. **52**, 403 (1969).

[6] A. J. Leggett, Can a solid be "superfluid"? Phys. Rev. Lett. **25**, 1543 (1970).

[7] G. V. Chester, Speculations on Bose-Einstein condensation and quantum crystals, Phys. Rev. A **2**, 256 (1970).

[8] S. Wessel and M. Troyer, Supersolid hard-core bosons on the triangular lattice, Phys. Rev. Lett. **95**, 127205 (2005).

[9] M. H. W. Chan, Supersolidity, Science **319**, 1207 (2008).

[10] S. Balibar, The enigma of supersolidity, Nature (London) **464**, 176 (2010).

[11] C. Cazorla, G. E. Astrakharchik, J. Casulleras, and J. Boronat, Ground-state properties and superfluidity of two- and quasi-two-dimensional solid ^{4}He, J. Phys.: Condens. Matter **22**, 165402 (2010).

[12] P. L. Silvestrelli, M. Nava, F. Ancilotto, and L. Reatto, Prediction for two spatially modulated superfluids: ^{4}He on fluorographene and on hexagonal BN, J. Low Temp. Phys. **196**, 42 (2019).

[13] P. A. Crowell and J. D. Reppy, Reentrant superfluidity in ^{4}He films adsorbed on graphite, Phys. Rev. Lett. **70**, 3291 (1993).

[14] M. Boninsegni, On the existence of supersolid ^{4}He monolayer films, J. Low Temp. Phys. **165**, 67 (2011).

[15] J. Nyéki, A. Phillis, A. Ho, D. Lee, P. Coleman, J. Parpia, B. Cowan, and J. Saunders, Intertwined superfluid and density wave order in two-dimensional ^{4}He, Nat. Phys. **13**, 455 (2017).

[16] J. Nyéki, A. Phillis, B. Cowan, and J. Saunders, On the "supersolid" response of the second layer of ^{4}He on graphite, J. Low Temp. Phys. **187**, 475 (2017).

[17] J. Knapp, J. Nyéki, H. Patel, F. Ziouzia, B. P. Cowan, and J. Saunders, Thermodynamic evidence for density wave order in a two dimensional ^{4}He supersolid, Phys. Rev. Lett. **134**, 096002 (2025).

[18] C. Wang, C. Gao, C.-M. Jian, and H. Zhai, Spin-orbit coupled spinor Bose-Einstein condensates, Phys. Rev. Lett. **105**, 160403 (2010).

[19] N. Henkel, R. Nath, and T. Pohl, Three-dimensional roton excitations and supersolid formation in Rydberg-excited Bose-Einstein condensates, Phys. Rev. Lett. **104**, 195302 (2010).

[20] S. Datta and S. Yarlagadda, Supersolidity for hard-core-bosons coupled to optical phonons, Solid State Commun. **150**, 2040 (2010).

[21] P. W. Anderson, Theory of supersolidity, J. Low Temp. Phys. **169**, 124 (2012).

[22] Y. Li, L. P. Pitaevskii, and S. Stringari, Quantum tricriticality and phase transitions in spin-orbit coupled Bose-Einstein condensates, Phys. Rev. Lett. **108**, 225301 (2012).

[23] G. Biagioni, N. Antolini, A. Alaña, M. Modugno, A. Fioretti, C. Gabbanini, L. Tanzi, and G. Modugno, Dimensional crossover in the superfluid-supersolid quantum phase transition, Phys. Rev. X **12**, 021019 (2022).

[24] Y.-C. Zhang and F. Maucher, Variational approaches to two-dimensionally symmetry-broken dipolar Bose–Einstein condensates, Atoms **11**, 102 (2023).

[25] J. Léonard, A. Morales, P. Zupancic, T. Esslinger, and T. Donner, Supersolid formation in a quantum gas breaking a continuous translational symmetry, Nature (London) **543**, 87 (2017).

[26] J.-R. Li, J. Lee, W. Huang, S. Burchesky, B. Shteynas, F. Ç. Top, A. O. Jamison, and W. Ketterle, A stripe phase with supersolid properties in spin–orbit-coupled Bose–Einstein condensates, Nature (London) **543**, 91 (2017).

[27] S. C. Schuster, P. Wolf, S. Ostermann, S. Slama, and C. Zimmermann, Supersolid properties of a Bose-Einstein condensate in a ring resonator, Phys. Rev. Lett. **124**, 143602 (2020).

[28] N. Liebster, M. Sparn, E. Kath, J. Duchene, H. Strobel, and M. K. Oberthaler, Supersolid-like sound modes in a driven quantum gas, Nat. Phys. **21**, 1064 (2025).

[29] L. Chomaz, D. Petter, P. Ilzhöfer, G. Natale, A. Trautmann, C. Politi, G. Durastante, R. M. W. van Bijnen, A. Patscheider, M. Sohmen, M. J. Mark, and F. Ferlaino, Long-lived and transient supersolid behaviors in dipolar quantum gases, Phys. Rev. X **9**, 021012 (2019).

[30] F. Böttcher, J.-N. Schmidt, M. Wenzel, J. Hertkorn, M. Guo, T. Langen, and T. Pfau, Transient supersolid properties in an array of dipolar quantum droplets, Phys. Rev. X **9**, 011051 (2019).

[31] L. Tanzi, S. M. Roccuzzo, E. Lucioni, F. Famà, A. Fioretti, C. Gabbanini, G. Modugno, A. Recati, and S. Stringari, Supersolid symmetry breaking from compressional oscillations in a dipolar quantum gas, Nature (London) **574**, 382 (2019).

[32] L. Tanzi, E. Lucioni, F. Famà, J. Catani, A. Fioretti, C. Gabbanini, R. N. Bisset, L. Santos, and G. Modugno, Observation of a dipolar quantum gas with metastable supersolid properties, Phys. Rev. Lett. **122**, 130405 (2019).

[33] M. Sohmen, C. Politi, L. Klaus, L. Chomaz, M. J. Mark, M. A. Norcia, and F. Ferlaino, Birth, life, and death of a dipolar supersolid, Phys. Rev. Lett. **126**, 233401 (2021).

[34] A. Alaña, I. L. Egusquiza, and M. Modugno, Supersolid formation in a dipolar condensate by roton instability, Phys. Rev. A **108**, 033316 (2023).

[35] A. Recati and S. Stringari, Supersolidity in ultracold dipolar gases, Nat. Rev. Phys. **5**, 735 (2023).

[36] N. Bigagli, W. Yuan, S. Zhang, B. Bulatovic, T. Karman, I. Stevenson, and S. Will, Observation of Bose–Einstein condensation of dipolar molecules, Nature (London) **631**, 289 (2024).

[37] E. P. Gross, Hydrodynamics of a superfluid condensate, J. Math. Phys. **4**, 195 (1963).

[38] I. N. Adamenko, K. E. Nemchenko, and I. V. Tanatarov, Transmission and reflection of phonons and rotons at the superfluid helium-solid interface, Phys. Rev. B **77**, 174510 (2008).

[39] Y. Pomeau and D. C. Roberts, Hydrodynamic boundary condition for superfluid flow, Phys. Rev. B **77**, 144508 (2008).

[40] D. C. Roberts, When superfluids are a drag, Contemp. Phys. **50**, 453 (2009).

[41] A. Ambrosetti, G. Palermo, and P. L. Silvestrelli, Quantum-mechanically enhanced water flow in subnanometer carbon nanotubes, J. Phys. Chem. C **126**, 20174 (2022).

[42] A. Ambrosetti, P. L. Silvestrelli, and L. Salasnich, Superfluidity meets the solid state: Frictionless mass transport through a (5,5) carbon nanotube, Phys. Rev. Lett. **131**, 206301 (2023).

[43] J. B. Pendry, Shearing the vacuum - quantum friction, J. Phys.: Condens. Matter **9**, 10301 (1997).

[44] B. N. J. Persson and Z. Zhang, Theory of friction: Coulomb drag between two closely spaced solids, Phys. Rev. B **57**, 7327 (1998).

[45] A. I. Volokitin and B. N. J. Persson, Theory of friction: The contribution from a fluctuating electromagnetic field, J. Phys.: Condens. Matter **11**, 345 (1999).

[46] A. I. Volokitin and B. N. J. Persson, Quantum field theory of van der Waals friction, Phys. Rev. B **74**, 205413 (2006).

[47] N. Kavokine, M.-L. Bocquet, and L. Bocquet, Fluctuation-induced quantum friction in nanoscale water flows, Nature (London) **602**, 84 (2022).

[48] B. Coquinot, M. Becker, R. R. Netz, L. Bocquet, and N. Kavokine, Collective modes and quantum effects in two-dimensional nanofluidic channels, Faraday Discuss. **249**, 162 (2024).

[49] A. T. Bui, F. L. Thiemann, A. Michaelides, and S. J. Cox, Classical quantum friction at water–carbon interfaces, Nano Lett. **23**, 580 (2023).

[50] M. Lizée, B. Coquinot, G. Mariette, A. Siria, and L. Bocquet, Anomalous friction of supercooled glycerol on mica, Nat. Commun. **15**, 6129 (2024).

[51] B. Coquinot, L. Bocquet, and N. Kavokine, Quantum feedback at the solid-liquid interface: Flow-induced electronic current and its negative contribution to friction, Phys. Rev. X **13**, 011019 (2023).

[52] B. Coquinot, L. Bocquet, and N. Kavokine, Hydroelectric energy conversion of waste flows through hydroelectronic drag, Proc. Natl. Acad. Sci. USA **121**, e2411613121 (2024).

[53] B. Coquinot, A. T. Bui, D. Toquer, A. Michaelides, N. Kavokine, S. J. Cox, and L. Bocquet, Momentum tunnelling between nanoscale liquid flows, Nat. Nanotechnol. **20**, 397 (2025).

[54] See Supplemental Material at http://link.aps.org/supplemental/10.1103/xfj1-gndb for detailed analytical derivations and numerical results.

[55] Y.-C. Zhang, F. Maucher, and T. Pohl, Supersolidity around a critical point in dipolar Bose-Einstein condensates, Phys. Rev. Lett. **123**, 015301 (2019).

[56] L. Salasnich, Self-consistent derivation of the modified Gross–Pitaevskii equation with Lee–Huang–Yang correction, Appl. Sci. **8**, 1998 (2018).

[57] T. G. Skov, M. G. Skou, N. B. Jørgensen, and J. J. Arlt, Observation of a Lee-Huang-Yang fluid, Phys. Rev. Lett. **126**, 230404 (2021).

[58] M. Boninsegni, N. Prokof'ev, and B. Svistunov, Superglass phase of ^{4}He, Phys. Rev. Lett. **96**, 105301 (2006).

[59] P. Corboz, M. Boninsegni, L. Pollet, and M. Troyer, Phase diagram of ^{4}He adsorbed on graphite, Phys. Rev. B **78**, 245414 (2008).

[60] L. Pollet, M. Boninsegni, A. B. Kuklov, N. V. Prokof'ev, B. V. Svistunov, and M. Troyer, Local stress and superfluid properties of solid ^{4}He, Phys. Rev. Lett. **101**, 097202 (2008).

[61] T. Bland, E. Poli, C. Politi, L. Klaus, M. A. Norcia, F. Ferlaino, L. Santos, and R. N. Bisset, Two-dimensional supersolid formation in dipolar condensates, Phys. Rev. Lett. **128**, 195302 (2022).

[62] K. Bertoldi, V. Vitelli, J. Christensen, and M. van Hecke, Flexible mechanical metamaterials, Nat. Rev. Mater. **2**, 17066 (2017).

[63] J. B. Berger, H. N. G. Wadley, and R. M. McMeeking, Mechanical metamaterials at the theoretical limit of isotropic elastic stiffness, Nature (London) **543**, 533 (2017).

[64] C. Chin, R. Grimm, P. Julienne, and E. Tiesinga, Feshbach resonances in ultracold gases, Rev. Mod. Phys. **82**, 1225 (2010).

[65] C. Zerba, C. Kuhlenkamp, L. Mangeolle, and M. Knap, Tuning transport in solid-state Bose-Fermi mixtures by Feshbach resonances, Phys. Rev. Lett. **134**, 126502 (2025).

[66] S. Marbach and L. Bocquet, Osmosis, from molecular insights to large-scale applications, Chem. Soc. Rev. **48**, 3102 (2019).